Adsorption (2013) 19:1137–1148
DOI 10.1007/s10450-013-9540-5

Adsorption of toluene and toluene–water vapor mixture on almond shell based activated carbons

A. Martínez de Yuso · M. T. Izquierdo · B. Rubio · P. J. M. Carrott

Received: 7 February 2012 / Accepted: 6 March 2013 / Published online: 16 March 2013

Abstract The aim of work is to study the adsorption of a common volatile organic compound such as toluene using activated carbons prepared by chemical activation with phosphoric acid of a lignocellulosic precursor, almond shell, under different conditions. The Impregnation ratio, temperature and time of activation were modified to obtain activated carbons with different characteristics. Regarding the characteristics of the activated carbons, the effects of porous structure and surface chemistry on the toluene adsorption capacity from toluene isotherms have been analysed. Results show that the control of properties of the activated carbons, particularly porous structure, highly dependent on the preparation conditions, plays a decisive role on the toluene adsorption capacity of the activated carbons. Concerning the experiments of toluene adsorption conducted in dynamic mode, activated carbons prepared at low temperatures of activation show higher breakthrough times than those obtained for activated carbons prepared at higher activation temperatures. The amount of toluene adsorbed in presence of water vapor in the gas stream lead to a decrease ranging from 33 to 46 % except for carbons prepared at higher temperatures activated that show only a slight decrease in the amount of toluene adsorbed. Activated carbons can be regenerated with soft heat treatment showing a slight decrease in the adsorption capacity. The high toluene adsorption capacities as well as the high breakthrough times obtained in presence of water vapor make these activated carbons suitable for commercial applications.

Keywords Adsorption · Activated carbon · Volatile organic compounds · Toluene · Water vapor · Almond shell · Phosphoric acid

1 Introduction

Organic solvents, such as acetone, benzene, toluene or xylene, are widely used in industrial processes like painting and coating. The emission of VOCs has very harmful effects for both human health and the environment. Headache, nausea, damage to the central nervous system or lung cancer may be caused by VOCs exposure (Jones 2002). VOCs also play an important role as precursors in the formation of photochemical smog (Sillman 2003).

Common methods to control VOCs emissions are condensation, adsorption, catalytic oxidation and thermal oxidation (Ruddy and Carroll 1993). Among the available alternatives, adsorption on activated carbon is an established technology widely used in industrial processes that permits not only the removal of VOCs but also their recovery from gas streams for reuse. Another advantage of the use of activated carbons is that it permits high removal efficiency at low inlet concentration. Many precursors can be used to prepare activated carbon, and nowadays one of the most important raw materials for their production are lignocellulosic materials.

A. Martínez de Yuso (✉)
Universidad San Jorge, Autovía A23 Zaragoza-Huesca km 510, Villanueva de Gállego, 50830 Zaragoza, Spain
e-mail: acmartinez@usj.es

M. T. Izquierdo · B. Rubio
Instituto de Carboquímica, CSIC, C/Miguel Luesma 4, 500018 Zaragoza, Spain

P. J. M. Carrott
Centro de Química de Évora, Colégio Luís António Verney, Rua Romão Ramalho, 7000-671 Évora, Portugal

The adsorption of some very common VOCs on activated carbon has been measured by a number of authors (Benkheda et al. 2000; Silvestre-Albero et al. 2009; Lillo-Rodenas et al. 2005; Bouhamra et al. 2009). But the study of the adsorption of these compounds in the presence of water vapor is less common (Cal et al. 1996). Since water vapor is present in many industrial process gas streams it is important to understand water vapor adsorption on activated carbon and its effects on VOCs adsorption, as water vapor can competitively adsorb on activated carbon (Lavanchi and Stoeckli 1999).

The goal of this study is the adsorption of a common volatile organic compound such as toluene using activated carbons prepared by chemical activation of a lignocellulosic precursor (almond shell). The effect of porous structure, surface chemistry and the presence of water vapor have been analysed in a series of activated carbons prepared under different conditions to identify the most adequate conditions to prepare activated carbons for VOCs adsorption.

With a view to reducing the cost of the preparation of the carbons, a low cost precursor has been selected and the preparation of the materials was carried out under moderate conditions of temperature, impregnation ratio and time of activation.

2 Experimental

2.1 Preparation of activated carbons

Almond shell produced in Vera del Moncayo, Zaragoza (Spain), was chosen as raw material for the preparation of the activated carbons. Dry shells were crushed and sieved at 0.2–1 mm. The chemical activation was carried out by impregnation of the almond shell with (*ortho*)-phosphoric acid of 89 wt% followed by one-step carbonization-activation in N_2 atmosphere.

Experimental conditions to prepare the activated carbons were obtained using an experimental design with a commercial software. A mixture design simplex based on a centroid design with interior points and two center runs was used. The three mixture variables introduced in the design were impregnation ratio (defined as: weight of phosphoric acid/weight of precursor), temperature and time of activation. The variables were defined as a continuous function in the range of 0.5–1.5, 400–800 °C and 30–120 min, respectively, giving a total of 12 experiments. More details of the experimental procedure are given in Izquierdo 2011.

From the 12 activated carbons prepared, under the different experimental conditions, some samples were selected on the basis of higher surface area. The activated carbons included in this study are given in Table 1.

Table 1 Preparation conditions of the activated carbons and labelling of samples

Sample	T (°C)	IR[a]	t (min)
AT400R1t75	400	1.00	75
AT467R117t45	467	1.17	45
AT533R083t60	533	0.83	60
AT533R083t60(2)	533	0.83	60
AT600R1t30	600	1.00	30
AT800R15t120	800	1.50	120

[a] Impregnation ratio: amount phosphoric acid (g)/amount almond shell (g)

2.2 Characterization of activated carbons

All activated carbons were chemically and structurally characterized by ultimate analysis, infrared spectroscopy (FTIR), temperature programmed desorption coupled to mass spectrometry (TPD-MS), thermogravimetry (DTG), point of zero charge (PZC), Boehm titrations and nitrogen adsorption at −196 °C.

Ultimate analysis of the activated carbons was carried out in a Thermo Flash 1112 microanalysis apparatus. Oxygen content was obtained by difference.

FTIR spectra were recorder using a Bruker Tensor 27 spectrophotometer 32 scans between 600–4,000 and 2 cm^{-1} of resolution.

The TPD runs were carried out with a custom build set-up, consisting of a tubular quartz reactor placed inside an electrical furnace connected to a quadrupole mass spectrometer from Pfeifer. TPD experiments were carried out by heating the samples in Ar flow up to 1,100 °C at a heating rate of 10 °C/min, and recording the amount of CO and CO_2 evolved at each temperature with the mass spectrometer. The calibrations for CO and CO_2 were carried out by standards diluted in Ar. For each experiment 0.5 g of activated carbon was placed in a horizontal quartz tube reactor under a stream of 30 ml/min of Ar.

Thermogravimetric curves were obtained using a TA Instruments thermobalance. In a typical run 20 mg of sample was placed in a Pt crucible and was heated al 10 °C/min until 1,000 °C under al flow of Ar.

The immersion technique (Babić et al. 1999) was used for determination of the PZC of the samples. Suspensions of 0.7 g of activated carbon were put in contact with 10 ml of $NaNO_3$ 0.1 M at different pH values. Initial pH values were obtained by adding an amount of HNO_3 or NaOH solution taking the $NaNO_3$ solution to pH 3, 6 and 10. The suspensions were agitated for 24 h in a shaker at 250 r.p.m. at room temperature and filtered. The pH of the filtered solutions were measured. The final values for the PZC were the average of the three pH values.

The Boehm titration method was used for determination of the oxygenated surface groups. An amount of 0.5 g of the activated carbon samples was immersed into 50 ml 0.1 M of NaOH, Na_2CO_3, $NaHCO_3$ and $NaOC_2H_5$ solutions (Boehm 1964). The suspensions were agitated for 24 h at room temperature and filtered. The filtered solutions were titrated with HCl 0.1 M. The amount of the oxygenated groups of the surface of the carbons was calculated from the amount of HCl that reacted with the carbon.

The nitrogen adsorption at −196 °C was carried out in a Micromeritics ASAP 2020 automatic adsorption apparatus. The samples were initially outgassed at 150 °C and up to a vacuum of 10^{-6} mmHg. The volume of adsorbed nitrogen was measured from a relative pressure of 10^{-7} up to 0.995. The isotherms were analysed using different methods such as the BET method for determination of surface area and the BJH method for determining the volume of mesopores. The total pore volume was taken from the measurement of adsorbed nitrogen at a relative pressure of 0.995. QSDFT pore side distributions were calculated from the nitrogen adsorption results using software from Autosorb, Version 1.55, Quantachrome.

3 Toluene and water adsorption

3.1 Static adsorption

The water adsorption isotherms were carried out in a custom built set-up consisting of a gravimetric balance, pressure transducer and a system made of glass with a water deposit. For a typical run among 100 mg of activated carbon was placed in the gravimetric balance and out gassed at 150 °C for 2 h. For obtaining the isotherm the temperature was kept constant al 25 °C using a thermostated bath.

The adsorption–desorption isotherms of toluene were determined gravimetrically using an automatic adsorption apparatus (VTI Co). The temperature of the sample, 25 °C, was monitored during the experiment and a pressure transducer monitored the pressure of the system. For each experiment 80 mg of activated carbon was taken. Initially the sample was outgassed at 150 °C and up to a vacuum of 10^{-6} mmHg. After cooling to 25 °C toluene was introduced in the system to obtain the adsorption and desorption isotherms.

To study the regenerability of the activated carbons adsorption cycles were made from one of the samples. The regeneration (desorption) of saturated carbons was carried out by heating the carbon at 150 °C to remove the toluene. Once constant weight was reached, a new adsorption isotherm was obtained.

3.2 Dynamic adsorption

The toluene dynamic adsorptions were carried out in a custom built set-up, consisting of a vertical tubular steel reactor, containing the sample, connected to a gas inlet system. A schematic diagram of the experimental set-up is shown in Fig. 1. An argon flow with a known toluene concentration passed through the sample and the VOC remaining concentration in the flow was measured with a quadrupole mass spectrometer from Pfeiffer. The calibration of toluene was carried out by standard diluted in Ar. For a typical experiment 0.5 g of the activated carbon was taken.

To study the effect of the presence of water vapor in toluene adsorption on activated carbon dynamic adsorptions of toluene were carried out in the presence of water vapor. An argon flow was passed through a saturator containing water at a fixed temperature to give 3 % water vapor.

4 Results and discussion

4.1 Characterization of samples

Ultimate analysis and yield of activated carbons (calculated as 100 × mass of AC/mass precursor) is included in Table 2. The activated carbons samples have low nitrogen content and a negligible amount of sulfur. It can also be observed that samples prepared at lower temperatures of activation have a higher content in hydrogen.

The surface chemistry of the samples was evaluated by FTIR and Boehm titrations. The analysis of the FTIR spectra is included in Fig. 2. Samples obtained at lower

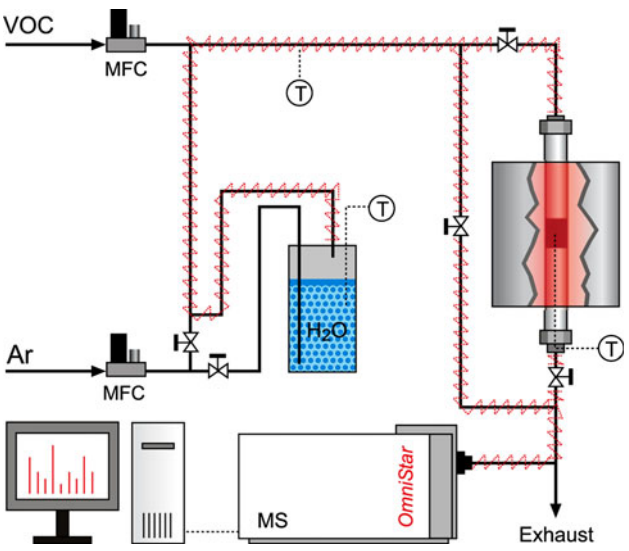

Fig. 1 Schematic diagram of the experimental set-up

Table 2 Chemical characterization of the activated carbons

Sample	Elemental composition (% in dry basis)					
	C	H	N	S	O[a]	Yield[b]
AT400R1t75	72.5	4.42	0.31	n	22.07	68.4
AT467R117t45	70	2.72	0.3	n	26.98	70.6
AT533R083t60	68.7	2.12	0.38	n	28.8	72.9
AT533R083t60(2)	68.11	2.57	0.5	n	28.82	73.6
AT600R1t30	68.47	2.05	0.42	n	29.06	73.2
AT800R15t120	71.44	1.93	0.37	n	26.26	67.3

n negligible

[a] By difference

[b] Mass of activated carbon/mass of precursor ×100

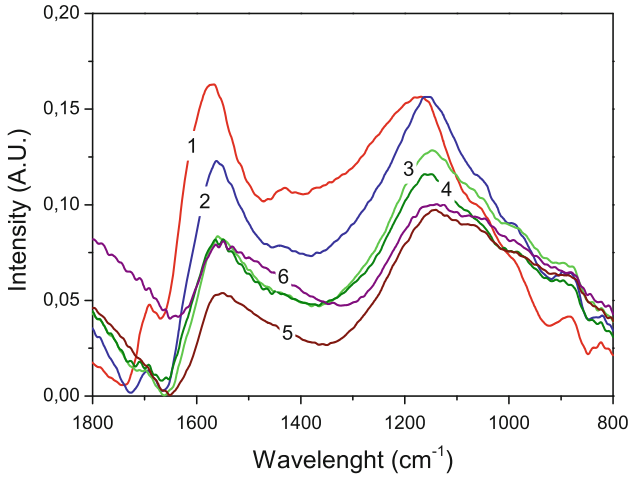

Fig. 2 FTIR spectra for activated carbon samples *1* AT400R1t75, *2* AT467R117t45, *3* AT533R083t60, *4* AT533R083t60(2), *5* AT600R 1t30 and *6* AT800R15t120

temperatures of activation have sharper bands than those of the samples obtained at higher temperatures. Small bands at around 1700 cm^{-1} are present only on samples activated at lower temperatures and they are usually caused by the stretching vibration of C=C in ketones, aldehydes, lactones and carboxyl groups. The low intensity of this band suggests little contribution of carboxyl group. This band disappears for activated carbons obtained at higher temperatures of activation. The band around 1600 cm^{-1} is attributed to aromatic ring or C=C stretching vibration. This indicates the formation of carbonyl-containing groups. Samples obtained at low temperatures of activation present a shoulder at 1400 cm^{-1} attributed to O–H bindings in lactones and carboxyl carbonates. This shoulder decreases in intensity at increasing temperature of activation up to complete disappearance. The existence of phenols is supported by O–H bending (1400 cm^{-1}) and C–O stretching (1200–1180 cm^{-1}) vibrations characteristic of phenols (Puziy et al. 2005). Bands around 1200 cm^{-1} are typical of P=O and P–O–C bonds (Puziy et al. 2002). This suggests the presence of phosphorus-containing groups. The relative intensity change of this band with activation temperature indicates the decrease of these groups at increasing activation temperature. Vibrations of C–H bonds in aromatic rings can be followed around wavelengths of 1000 cm^{-1}. These vibrations are clearly found in samples obtained at higher temperatures of activation and are shifted to higher wavelengths. This indicates less aromatic carbons at lower temperatures of activation with contribution of symmetrical bending of C–H bond in methyl groups.

The PZC is a very useful parameter in sorption studies that allows one to hypothesise on the ionization of functional groups and their interactions with adsorbates. PZC is defined as the value of pH at which the sorbent surface charge takes a zero value (Noh and Schwarz 1988, 1990; Bandosz et al. 1993; Carrott 1995).

PZC of the activated carbons can be seen in Table 3. All samples have noticeably acid properties with PZC values between 1.74 and 4.04 which is explained by the formation of acidic groups at the carbon surface as a result of the activating agent used. These results are in agreement with the results obtained by FTIR analysis and Boehm titrations. Differences in results are a consequence of different parameters of preparation which confirms that, by carefully selecting the conditions of preparation, it is possible to prepare activated carbon with different acidity levels and oxygen surface groups distribution (Menéndez and Illán-Gómez 1995). It can be observed that the values obtained for PZC decrease when the temperature of activation is increased.

To determine the effect of the conditions of activation on the formation of functional surface groups, Boehm titration was performed on activated carbons prepared in this study. It is assumed that sodium bicarbonate neutralizes carboxylic acids; sodium carbonate neutralizes both carboxylic acids and lactones; sodium hydroxide neutralizes lactones, whereas sodium ethoxide reacts with carbonyl acids. From Table 3, it can be seen that increasing the temperature of activation increases the amount of acidic groups, carboxylic and carbonyl groups. These groups can be formed during cooling of the activated carbon after the heating process. This cooling process enables the fixation of oxygen in the active sites (Boehm 1994). For all samples studied the amount of acidic groups is higher than that of basic groups. These results are in agreement with the acidic values obtained for PZC.

Studying together PZC and functional groups obtained by Boehm titrations a relationship between acid groups (expressed as the addition of the carbonyl and carboxylic groups) and the value of PZC has been found, and is shown in Fig. 3.

Table 3 Surface chemical characterization

Sample	PZC	Functional groups obtained by Boehm titration (mmol/g)				Total amount of CO and CO_2 evolved in TPD experiments (mmol/g)	
		Carboxylic	Phenolic	Carbonyl	Lactone	CO	CO_2
AT400R1t75	4.04	0.350	0.988	2.013	0.850	2.17	1.32
AT467R117t45	3.39	0.450	1.100	2.175	0.650	2.18	1.18
AT533R083t60	2.36	0.450	0.875	2.625	0.800	2.23	0.39
AT533R083t60(2)	1.89	0.450	1.025	2.400	0.900	2.18	0.36
AT600R1t30	1.89	0.475	0.975	2.425	0.750	3.04	0.45
AT800R15t120	1.79	0.525	1.000	2.425	1.075	3.72	1.29

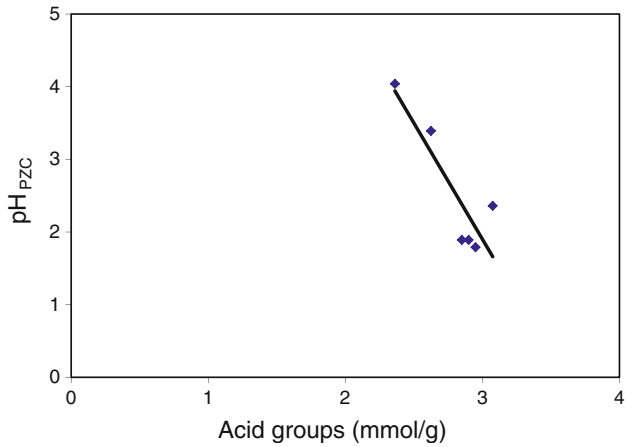

Fig. 3 PZC versus acid groups calculated by Boehm titrations

The quantification of TPD results is included in Table 3 and the profiles of CO and CO_2 obtained are shown in Fig. 4. During the thermal decomposition of the surface complexes, CO_2 evolves from carboxylic groups and their derivatives, such as lactones and anhydrides, while CO is mainly a decomposition product of quinones, hydroxyquinones and phenols (Macías-Pérez et al. 2008; Figueiredo et al. 1999). The total amount of CO evolved during the thermal treatment is higher than the total amount of CO_2 for all the samples studied. Increasing the temperature of activation the amount of CO evolved increases, but there is no relationship with the amount of CO_2. The impregnation ratio and the time of activation are important parameters in the formation of oxygen superficial groups that evolve CO_2. The variation of the preparation conditions leads to activated carbon with different TPD spectra, not only in the amount evolved but also in the shape of the peaks of CO and CO_2.

The profiles of CO of samples obtained at lower temperatures of activation show two peaks centered at about 600 and 800 °C. The first peak can be attributed to lactones with contribution of phenolic and ether groups (Daifullah and Girgis 2003). The sample prepared at 533 °C exhibit

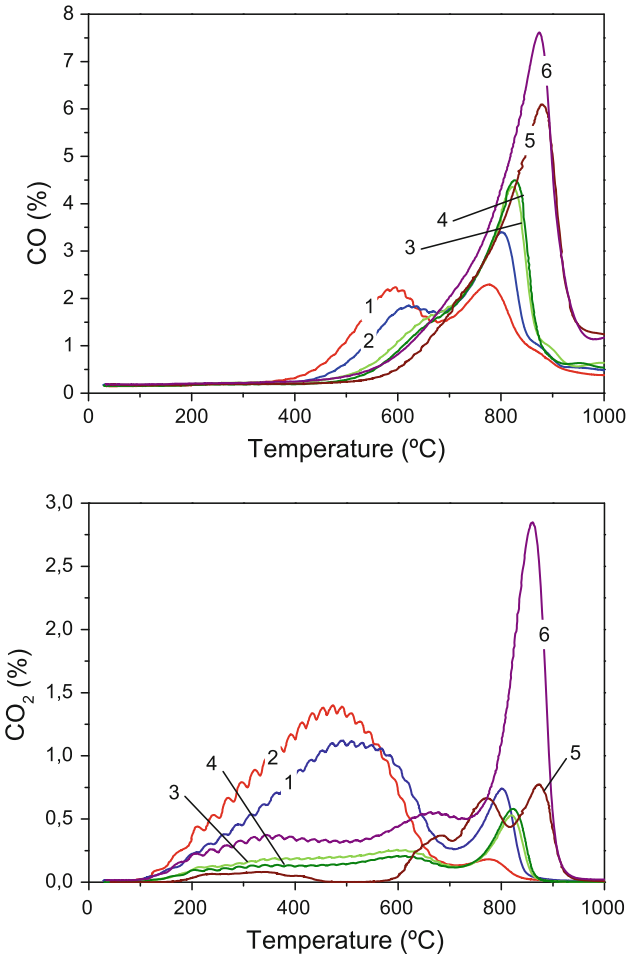

Fig. 4 Profiles of CO and CO_2 evolved in TPD experiments. Samples: *1* AT400R1t75, *2* AT467R117t45, *3* AT533R083t60, *4* AT533R083t60(2), *5* AT600R1t30 and *6* AT800T15t120

only a shoulder at 600 °C. This peak becomes smaller and displaced to higher temperatures for samples prepared at higher temperatures of activation. The second peak, near 800 °C, is an intense peak that can be attributed to anhydrides, carbonyls and quinones decomposition. This peak showed higher intensity increasing the temperature of

activation. The peak exhibits asymmetry at low temperatures, indicating a small contribution of phenols and ethers.

The profiles of CO_2 of samples obtained at lower temperatures of activation show two peaks. The first peak around 500 °C can be attributed to lactones with contribution of carboxyls. The second peak around 800 °C can be attributed to anhydrides. Increasing the temperature of activation of the samples the intensity of this peak increases. The sample obtained at 400 °C exhibits only a small shoulder not a well-defined peak at 800 °C, indicating that more stable functional groups are only formed at increasing the temperature of activation. Samples obtained at medium and higher temperatures of activation (533–800 °C) show a low intensity band up to approximately a temperature of desorption of 600 °C, indicating the disappearance of less stable functional groups, such as carboxyls and lactones.

Similar temperatures of evolution of the second peak of CO and CO_2 profiles are obtained. However the shape and the intensity changes because of the contribution of other surface complexes rather than anhydrides. The contribution of carbonyl and quinone-like groups seems to be higher for samples obtained at 467 and 533 °C, indicating the presence of more stable oxygen functional groups at increasing temperature of activation. The intensity of the peak obtained at temperatures near 800 °C for the CO profile is twice that of the CO_2 peak, attributed to anhydrides, indicating the presence of thermally stable groups such as quinones and carbonyls.

The shoulder obtained at 1,400 cm^{-1} on the FTIR spectra is consistent with results obtained by TPD when following CO_2 evolution for carbons obtained at lower activation temperatures.

Figure 5 depicts DTG curves of the samples. The thermal degradation characteristics of activated carbons prepared from lignocellulosic material are profoundly influenced by the chemical composition of the precursor (Antal and Varhegyi 1995). Lignocellulosic materials are mainly composed of cellulose, hemicellulose and lignin (Balci et al. 1993). Extractives and ash are present in the composition of those materials in a lower proportion (Ouensanga et al. 2003; Caballero et al. 1997). Decomposition of almond shell starts at 200 °C and is practically completed al 425 °C. Hemicellulose is the lighter fraction and decomposes at low temperatures (310 °C) while cellulose decomposes at higher temperature (at around 380 °C) (Font et al. 1991; Caballero et al. 1997). Lignin starts to decompose at low temperature (220 °C) and at low rate up to about 900 °C overlapping with the temperatures of decomposition of hemicellulose and cellulose (González et al. 2009). The addition of chemicals to almond shell and the thermal treatment carried out to prepare the activated carbons result in a variation in the temperature of decomposition in function of the employed conditions (Font et al. 1991; Suárez-García et al. 2004) shifting degradation to considerably higher temperatures (Girgis and Hendawy 2002).

The curves of DTG obtained do not present the processes corresponding to the decomposition of the hemicellulose and cellulose. This can be explained because the temperature used to prepare the activated carbons is higher than the decomposition temperature of hemicellulose and cellulose. The activated carbons prepared at lower temperatures (400–467 °C) present a broad band around 550 °C, which can indicate that the degradation process of the lignin has been incomplete. At increasing temperature of activation the band at about 800 °C becomes more intense and it is shifted to higher temperatures of decomposition. This band can indicate that the crosslinking process to produce aromatic units becomes important. At temperatures of activation of 600 and 800 °C the crosslinking process has started during activation of the samples and during TGA experiments this process is completed at temperatures around 900 °C.

Nitrogen isotherms of the activated carbons are given in Izquierdo 2011. The analysis of the nitrogen isotherms was performed using different approaches, namely, Brunauer–Emmet–Teller (BET), BJH method, t-plot method and DFT method. The percentage of microporosity was obtained as the ratio between total micropore volume, calculated applying the Dubinin–Radushkevich equation (Dubinin 1989) to the adsorption branch of the N_2 isotherm and the volume adsorbed at relative pressure of 0.995 (Lillo-Rodenas et al. 2005). The effect of the conditions of preparation on the BET surface area, micropore volume, total pore volume and the percentage of microporosity are given in Table 4.

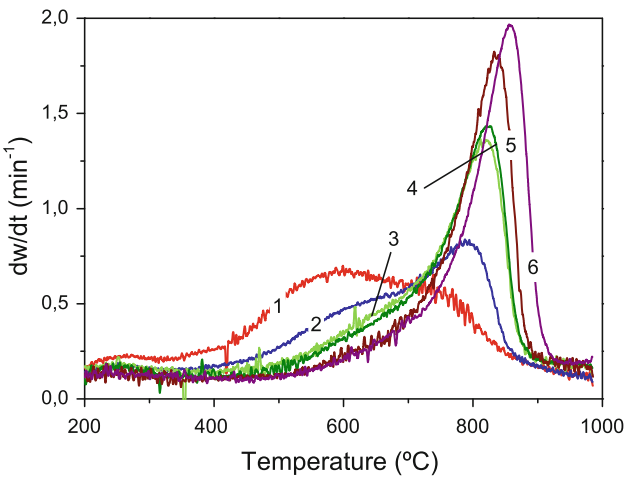

Fig. 5 DGT curves for decomposition of the samples. Samples: *1* AT40 0R1t75, *2* AT467R117t45, *3* AT533R083t60, *4* AT533R083T60(2), *5* AT600T1t30 and *6* AT800R15t120

Table 4 Results from N_2 physisorption

Sample	SBET (m^2/g)	Vmeso[a] (cm^3/g)	Vmicro[b] (cm^3/g)	Vp (p/p0 = 0.995) (cm^3/g)	Microporosity[c] (%)	MPW[d] (nm)
AT400R1t75	1,128 ± 50	0.385	0.259	0.67	77.8	1.154
AT467R117t45	1,117 ± 44	0.494	0.181	0.724	70.9	1.221
AT533R083t60	891 ± 36	0.341	0.194	0.571	74.6	1.602
AT533R083t60(2)	903 ± 36	0.378	0.182	0.593	72.0	1.680
AT600R1t30	926 ± 37	0.375	0.182	0.624	69.7	1.146
AT800R15t120	990 ± 38	0.511	0.145	0.694	64.6	1.964

[a] BJH method

[b] t-plot method

[c] According to Lillo-Rodenas et al. (2005)

[d] Median pore width HK method

BET surface area reaches highest values in samples prepared at lower temperatures (400–467 °C) with intermediate range of impregnation ratio (1.0–1.17) and intermediate times of activation (45–75 min) which is also verified for the micropore and mesopore volume calculated. This is in agreement with the results of Corcho-Corral et al. (2006) who obtained higher BET surface area at temperatures of activation of 400–450 °C using H_3PO_4 as activating agent.

The QSDFT method has been used to obtain the pore size distribution of the samples due to the advantages of the application of this method to micro-mesoporous activated carbons (Neimark et al. 2009). The data shown in Fig. 6 confirms the existence of a limited pore size distribution for all the samples (Valente Nabais et al. 2011). Samples show pores mainly in the micropore range centered at 1 nm. Increasing temperature of activation decreases the value of micropores (<2 nm) obtained for the samples. This indicates that the microporosity is developed at lower temperatures of activation (400–467 °C). At higher temperatures of activation the microporosity is not completely developed and a slight widening of the pores occurs.

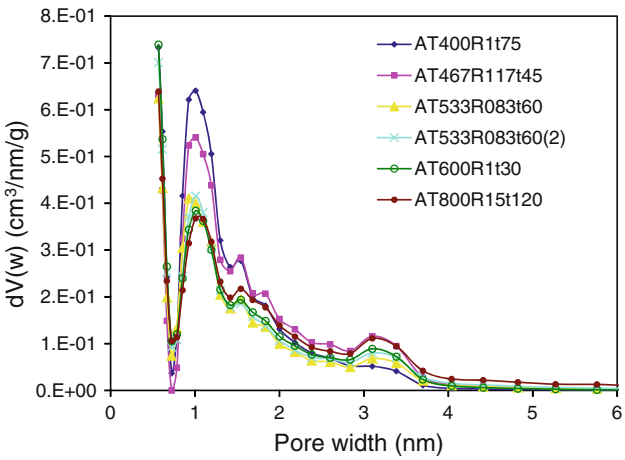

Fig. 6 QSDFT pore size distribution of the samples

4.2 Toluene and water adsorption

Several research works have been made about adsorption of water vapor due to the vulnerability of microporous activated carbons to humidity (Brennan et al. 2001). Although activated carbons have more affinity by VOCs than for water vapor, the presence of water vapor decreases the capacity of adsorption for VOCs of the activated carbons (Lavanchi and Stoeckli 1999), especially with high values of humidity. Water vapor process adsorption depends on the pore size distribution and surface groups (Alcañiz-Monge et al. 2002; Salame and Bandosz 1999a, b). But a qualitative difference exists between VOCs and water adsorption due to the different nature of the interactions that produce the adsorption. VOCs adsorption is produced by the dispersion forces but water adsorption is more complex compared with conventional adsorbates (N_2, CO_2, benzene). This is due to the weak dispersion interactions of the water with the carbon and the tendency of the water to form hydrogen bonds with the surface groups and other adsorbed water molecules. There are two main theories to explain water adsorption onto carbon materials. The first of them is based on the existence of a hysteresis loop in the adsorption isotherms, which is normally associated with the mechanism of capillary condensation (Alcañiz-Monge et al. 2001). In the second theory water adsorption occurs according to the Dubinin–Serpinski concept (Dubinin and Serpinsky 1981), by formation of clusters of water molecules on the primary adsorption centers. These centers are oxygenated compounds on the surface of the carbon that add water molecules by the creation of hydrogen bonds in a first stage of adsorption at low pressures. Each water molecule adsorbed is then a secondary adsorption center capable of forming hydrogen bonds with other molecules and creating clusters. Finally an increase in the pressure permits the growth of the clusters and the filling of

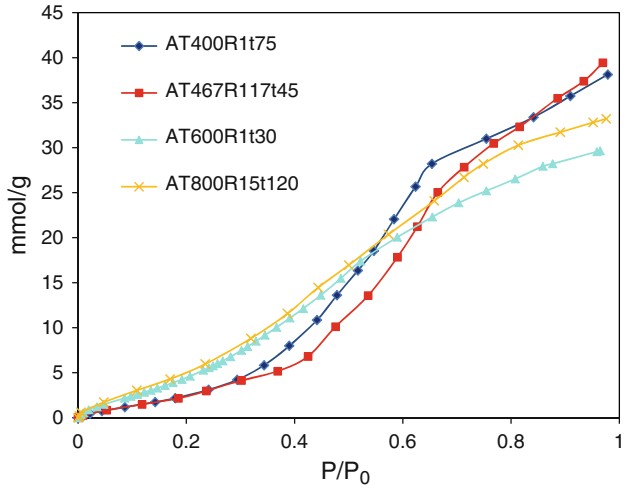

Fig. 7 H_2O adsorption isotherms

the pores by capillary condensation (Dubinin 1980; Brennan et al. 2001).

Adsorption equilibrium data for water vapor adsorption are represented graphically in Fig. 7. Water adsorption resulted in isotherms of type V according to the IUPAC classification, in agreement with results expected for porous carbons (Brennan et al. 2001). All water isotherms present hysteresis, which is usually interpreted by different filling and emptying mechanisms. The hysteresis phenomenon can be explained by the condensation of water vapor in the mesopores of the activated carbons (Lagorsse et al. 2005). The area of the hysteresis loop in the water isotherms obtained is larger than the area in the N_2 isotherm according to Naono and Hakuman (1993). The large hysteresis loop in the water isotherms indicates that both pore size and surface properties of the activated carbons have important effects on the hysteresis.

For all samples the amount of adsorbed N_2 is higher than the amount of adsorbed water for the maximum adsorption capacity in spite of the size of N_2 being higher than that of H_2O. This is in agreement with Alcañiz-Monge et al. (2002), Do and Do (2000) and Cossarutto et al. (2001). These results are shown in Table 5.

The model proposed by Dubinin–Serpinski is used to model the water vapor isotherms (Dubinin and Serpinsky 1981). Table 5 shows the results of the number of primary adsorption centers (a_o) and saturation adsorption (a_s) for the model.

A clear tendency between the amount of adsorbed water and the BET surface area exists. At increasing BET surface area the amount of water adsorbed increases. Comparing water adsorption with the total surface groups obtained by Boehm titrations, the samples with higher water adsorption capacities are the samples with lower surface groups content.

It can be concluded that the existence of oxygenated surface groups is important for water adsorption due to the fact that they act as primary adsorption centers adding water molecules to form clusters. But from above a certain value increasing oxygenated surface groups does not increase the water capacity adsorption for the samples. A good relationship between the amount of water adsorbed and the BET surface is obtained. This indicates that the growth of the clusters permits the filling of the carbon pores and at higher BET surface higher water adsorption capacities are obtained. Therefore the microporosity of the activated carbons seems to play the main role in the water adsorption for the activated carbons prepared in this study.

The static adsorption isotherms for toluene at 25 °C are shown in Fig. 8. The adsorption capacity, defined as the amount at the plateau of the isotherm, is higher for the samples prepared at lower temperatures (400–467 °C). The sample with lower adsorption capacity is the sample prepared at 533 °C which is the sample with the lower impregnation ratio. The samples prepared at 600 and 800 °C show also high adsorption capacities.

Comparing the amount of toluene adsorbed with BET surface area it can be concluded that samples with higher values of BET surface area obtain higher values of toluene adsorbed. However, there is not a direct correlation between the amount of toluene adsorbed and the BET

Table 5 Toluene and water static adsorption

Sample	Water adsorption				Toluene adsorption		
	Maximum capacity adsorption		Serpinski–Dubinin Model		Maximum capacity adsorption (mmol/g)	Langmuir Model	
	H_2O (cm^3/g)	N_2 (cm^3/g)	a_o (mmol/g)	a_s (mmol/g)		W_m (mmol/g)	K (cm^3/g)
AT400R1t75	0.687	0.700	1.728	38.821	6.612	6.54	1.21
AT467R117t45	0.711	0.724	2.628	40.735	6.924	6.89	0.94
AT533R083t60	–	–	–	–	4.954	4.95	1.51
AT533R083t60(2)	–	–	–	–	4.743	4.75	1.49
AT600R1t30	0.534	0.624	5.714	30.690	6.471	6.50	0.80
AT800R15t120	0.598	0.694	8.535	35.167	6.292	6.10	0.66

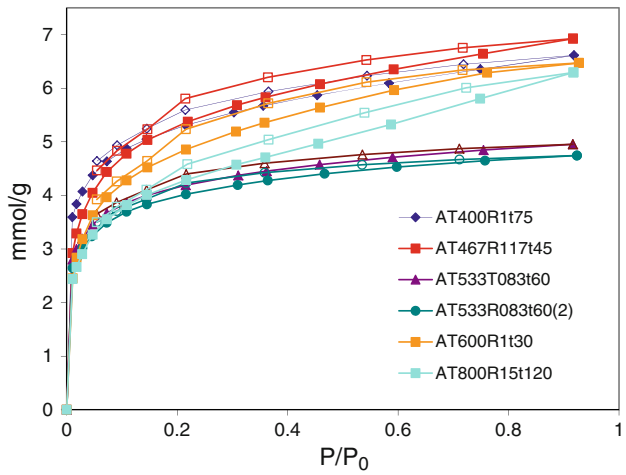

Fig. 8 Static adsorption capacity of activated carbons for toluene at 25 °C

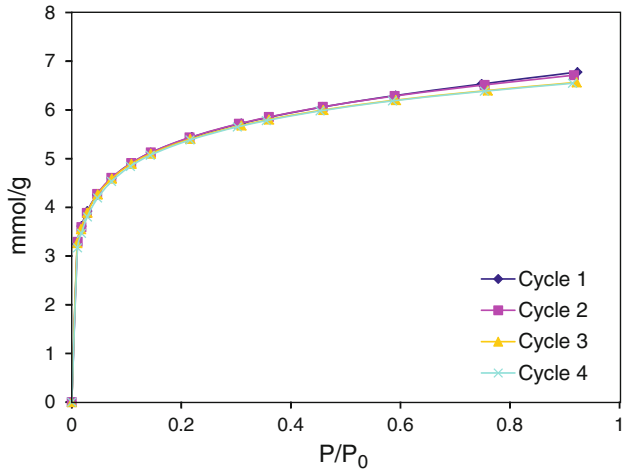

Fig. 9 Cycles of adsorption isotherms of toluene adsorption at 25 °C for sample AT467R117t45

surface. This indicates that both textural characteristics and surface chemistry have influence on adsorption capacity.

The experimental adsorption isotherm data were fitted to the Langmuir model (Langmuir 1918). The Langmuir isotherm expressed relatively well the adsorption of toluene, indicating the dependence on both physical and chemical adsorption. The parameters of limiting value for vapor adsorption (W_m) and constant value (K) obtained are summarized in Table 5. W_m has a good correlation with the experimental results obtained for toluene adsorption. Values of K can be related with the development of the microporosity of the activated carbons.

The ability to keep its adsorption capacity after successive adsorption and desorption cycles is one of the main characteristics of a good adsorbent. What is more, the recovery of the adsorbed VOC can be an added value allowing the reutilization of the VOC as raw material. Figure 9 shows the toluene adsorption cycles for the sample AT467R117t45. As observed in the figure, the sample exhibits a slight decrease in the amount adsorbed, but high toluene adsorption capacities are maintained through the four cycles studied. This fact can be due to the heating step before each subsequent cycle. These results make the activated carbons suitable for commercial applications.

The results in Table 6 show an important decrease in the amount of toluene adsorbed with 3 % of humidity. This is in agreement with studies carried out to understand the effect of relative humidity (RH) on the adsorption of VOCs on activated carbons. In the case of acetone, RH has little effect on the adsorption capacity on activated carbon cloth. In contrast the effect of RH on benzene adsorption has little effect below 65 %, the point at which capillary condensation of water vapor occurs in the pores (Cal et al. 1996). Werner (1985) observed that the amount of trichloroethylene adsorbed in his study decreased with increasing humidity concluding that this effect is most marked for high values or RH and low VOC concentration. In contrast Bouhamra et al. (2009), obtained a significant decrease in the amount of 1,1,1-trichloroethane adsorbed on activated carbon for low RH (0–30 %).

Samples with higher dynamic toluene adsorption at 500 ppm present higher decreases in the amount of toluene adsorbed in the presence of humidity. The decrease in the amount of toluene adsorbed varies between 33 and 46 %. Except for the sample prepared at more extreme conditions that presents a decrease of 9 %. The great decrease in the

Table 6 Dynamic toluene adsorption (mmol/g) 500 ppm and 3 % H_2O

Sample	Toluene 500 ppm		Toluene 500 ppm + 3 % H_2O	
	Sat (mmol/g)	20 % sat (mmol/g)	Sat (mmol/g)	20 % sat (mmol/g)
AT400R1t75	2.9942	2.8562	1.8591	1.8082
AT467R117t45	2.4982	2.3312	1.6654	1.3827
AT533R083t60	2.4210	2.2559	1.5255	1.2743
AT533R083t60(2)	2.2570	2.1422	1.3334	0.9541
AT600R1t30	2.5224	2.3799	1.3513	1.1369
AT800R15t120	1.8816	1.7647	1.7198	1.2510

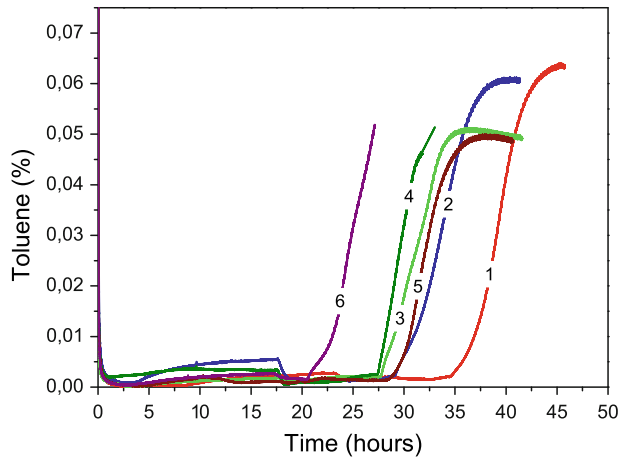

Fig. 10 Breakthrough curves for toluene 500 ppm adsorption over 0.5 g of the activated carbons. Samples: *1* AT400R1t75, *2* AT467R117t45, *3* AT533R083t60, *4* AT533R083t60(2), *5* AT600R1t30 and *6* AT800R15t120

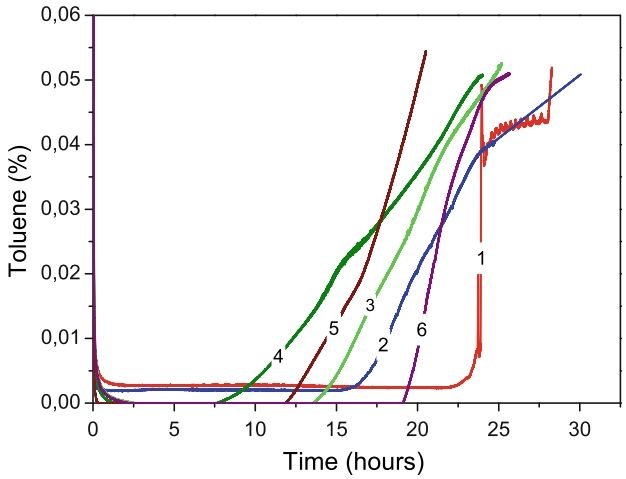

Fig. 11 Breakthrough curves for toluene 500 ppm and 3 % humidity over 0.5 g of activated carbons. Samples: *1* AT400R1t75, *2* AT467R117T45, *3* AT533R083t60, *4* AT533R083t60(2), *5* AT600R1t30 and *6* AT800T15t120

mass of toluene adsorbed in the presence of water vapor is most likely because toluene is insoluble and hydrophobic.

Figures 10 and 11 show breakthrough curves for toluene 500 ppm adsorption without and with humidity respectively. When adsorption was carried out without humidity, activated carbons prepared at lower temperatures of activation show higher times of breakthrough. Samples prepared at more extreme conditions present the lowest time of breakthrough.

The presence of humidity decreases the breakthrough times for toluene adsorption for all samples studied. The decrease varies from around 30 % for samples prepared at lower temperatures of activation and at more extreme conditions to 60–70 % for samples prepared at medium temperatures.

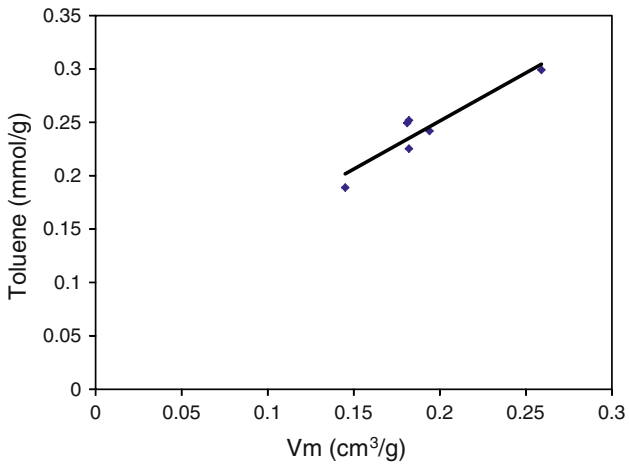

Fig. 12 Relationship between toluene adsorbed in dynamic adsorption at 500 ppm and the volume of micropores calculated by N_2 adsorption (at 77 K)

The shapes of the breakthrough curves are different for adsorption carried out in presence of water, with the curves being softer, except for sample AT400R1t75 which presents a more abrupt curve.

The results obtained show that the sample with the higher value of BET surface area presents the higher toluene adsorption capacity. It can be observed that maximum adsorption capacity for toluene is higher at increasing the BET surface area. In the case of toluene adsorption in the presence of humidity a relationship with BET surface area is found. No relationship with oxygenated functional groups has been observed in this study.

Figure 12 shows that a better relationship is obtained when the volume of micropores calculated by N_2 adsorption is used to compare the dynamic adsorption of toluene at 500 ppm. This is in agreement with Lillo-Rodenas et al. (2005) who found a relationship between the toluene adsorption and the volume of micropores calculated by N_2 and CO_2 adsorption.

5 Conclusions

Activated carbons with high adsorption capacities for toluene at low concentrations can be obtained by chemical activation with H_3PO_4 of almond shell. Changing the experimental variables of the preparation of the activated carbons the porosity can be tailored. Activated carbons prepared showed good surface characteristics with a well developed microporous structure.

Toluene adsorptions carried out over the activated carbons show that the amount of toluene adsorbed depends on

the porosity. BET surface area and micropore volume are the major parameters for toluene adsorption. The presence of 3 % of humidity in the flow decreases the amount of toluene adsorbed by 9–46 % depending on the sample. Activated carbons can be regenerated by heat treatment at 150 °C showing only a slight decrease of the adsorption capacity.

References

Alcañiz-Monge, J., Linares-Solano, A., Rand, B.: Water adsorption on activated carbons: study of water adsorption in micro- and mesopores. J. Phys. Chem. B **105**, 7998–8006 (2001)

Alcañiz-Monge, J., Linares-Solano, A., Rand, B.: Mechanism of adsorption of water in carbon micropores as revealed by a study of activated carbon fiber. J. Phys. Chem. B **106**, 3209–3216 (2002)

Antal, M.J., Varhegyi, G.: Cellulose pyrolysis kinetics: the current state of knowledge. Ind. Eng. Chem. Res. **34**, 703–717 (1995)

Babić, B.M., Milonjić, S.K., Polovina, M.J., Kaludierović, B.V.: Point of zero charge and intrinsic equilibrium constants of activated carbon cloth. Carbon **37**, 477–481 (1999)

Balci, S., Doğu, T., Yücel, G.: Pyrolysis of lignocellulosic materials. Ind. Chem. Res. **32**, 2573–2579 (1993)

Bandosz, T.J., Jagiello, J., Contescu, C., Schwarz, J.A.: Characterization of the surfaces of activated carbons in terms of their acidity constant distribution. Carbon **31**(7), 1193–1202 (1993)

Benkheda, J., Jaubert, J.N., Barth, D.: Experimental and modelled results describing the adsorption of toluene onto activated carbon. J. Chem. Eng. Data **45**, 653–661 (2000)

Boehm, H.P., Heck, W., Sappok, R., Diehl, E.: Surface oxides of carbon. Angew. Chem. Int. Ed. **3**(10), 669 (1964)

Boehm, H.P.: Some aspects of the surface chemistry of carbon blacks and other carbons. Carbon **32**, 759–769 (1994)

Bouhamra, W.S., Baker, C.G.J., Elkilani, A.S., Alkandari, A.A., Al-Masour, A.A.A.: Adsorption of toluene and 1,1,1-trichloroethane on selected adsorbents under a range of ambient conditions. Adsorption **15**, 461–475 (2009)

Brennan, J.K., Bandosz, T.J., Thomson, K.T., Gubbins, K.E.: Water in porous carbons. Colloid Surf. A Physicochem. Eng. Aspects **187**, 539–568 (2001)

Caballero, J.A., Conesa, J.A., Font, R., Marcilla, A.: Pyrolysis kinetics of almond shells and olive stones considering their organic fractions. J. Anal. Appl. Pyrolysis **42**, 159–175 (1997)

Cal, M.P., Rood, M.J., Larson, S.M.: Removal of VOCs from humidified gas stream using activated carbon cloth. Gas Sep. Purif. **10**(2), 117–121 (1996)

Carrott, P.J.M., Ribeiro Carrott, M.M.L., Estevão Candelas, A.J., Prates Ramalho, J.P.: Numerical simulation of surface ionisation and specific adsorption in a two-site model of a carbon surface. J. Chem. Soc. Faraday Trans. **91**(14), 2179–2184 (1995)

Cossarutto, L., Zimny, T., Kaczmarczyk, J., Siemieniewska, T., Bimer, J., Weber, J.V.: Transport and sorption of water vapour in activated carbons. Carbon **30**, 2339–2346 (2001)

Corcho-Corral, B., Olivares-Marín, M., Fernández-González, C., Gómez-Serrano, V., Macías-García, A.: Preparation and textural characterization of activated carbon from vine shoots (*Vitis vinifera*) by H_3PO_4-chemical activation. Appl. Surf. Sci. **252**, 5961–5966 (2006)

Daifullah, A.M.M., Girgis, B.B.: Impact of surfaces characteristics of activated carbon on adsorption of BTEX. Colloids Surf. A Physicochem. Eng. Aspects **214**, 181–193 (2003)

Do, D.D., Do, H.D.: A model for water adsorption in activated carbon. Carbon **38**(5), 767–773 (2000)

Dubinin, M.M.: Water vapour adsorption and the microporous structures of carbonaceous adsorbents. Carbon **18**, 355–364 (1980)

Dubinin, M.M., Serpinsky, V.V.: Isotherm equation for water vapour adsorption by microporous carbonaceous adsorbents. Carbon **19**(5), 402–403 (1981)

Dubinin, M.M.: Fundamentals of the theory of adsorption in micropores of carbon adsorbents—characteristics of their adsorption properties and microporous structure. Carbon **27**, 457–467 (1989)

Figueiredo, J.L., Pereira, M.F.R., Freitas, M.M.A., Órfão, J.J.M.: Modification of the surface chemistry of activated carbons. Carbon **37**, 1379–1389 (1999)

Font, R., Marcilla, A., Verdú, E., Devesa, J.: Thermogravimetric kinetic study of the pyrolysis of almond shells and almond shells impregnated with CoCl2. J. Anal. Appl. Pyrolysis **21**, 249–264 (1991)

Girgis, B.B., Hendawy, A.A.N.: Porosity development in activated carbons obtained from date pits under chemical activation with phosphoric acid. Microporous Mesoporous Mater. **52**, 105–117 (2002)

González, J.F., Román, S., Encinar, J.M., Martínez, G.: Pyrolysis of various biomass residues and char utilization for the production of activated carbons. J. Anal. Appl. Pyrolysis **85**, 134–141 (2009)

Izquierdo, M.T., Martínez de Yuso, A., Rubio, B., Pino, M.R.: Conversion of almond shell to activated carbons: methodical study of the chemical activation based on an experimental design and relationship with their characteristics. Biomass Bioenergy **35**, 1235–1244 (2011)

Jones, A.P.: Indoor air quality and health. In: Austin, J., Brimblecombe, P., Sturges, W. (eds.) Developments in Environmental Science. Elsevier, Amsterdam (2002)

Macías-Pérez, M.C., Lillo-Ródenas, M.A., Bueno-López, A., Salinas-Martínez de Lecea, C., Linares-Solano, M.: SO_2 retention on CaO/activated carbon sorbents. Part II: effect of the activated carbon support. Fuel **87**, 2544–2550 (2008)

Menéndez, J.A., Illán-Gómez, M.J., León y León, C.A., Radovic, L.R.: On the difference between the isoelectric point and the point of zero charge of carbons. Carbon **33**(11), 1655–1659 (1995)

Lagorsse, S., Campo, M.C., Magalhaes, F.D., Mendes, A.: Water adsorption on carbon molecular sieve membranes: experimental data and isotherm model. Carbon **43**, 2769–2779 (2005)

Langmuir, I.: The adsorption of gases on plane surfaces of glass, mica and platinum. J. Am. Chem. Soc. **40**, 1361–1402 (1918)

Lavanchi, A., Stoeckli, F.: Dynamic adsorption, in active carbon beds, of vapour mixtures corresponding to miscible and immiscible liquids. Carbon **37**(2), 315–321 (1999)

Lillo-Rodenas, M.A., Cazorla-Amoros, D., Linares-Solano, A.: Behaviour of activated carbons with different pore size distributions and surface oxygen groups for benzene and toluene adsorption at low concentration. Carbon **43**, 1758–1767 (2005)

Naono, H., Hakuman, M.: Analysis of porous texture by means of water vapour adsorption isotherm with particular attention to lower limit of hysteresis loop. J. Colloid Interface Sci. **158**, 19–26 (1993)

Neimark, A.V., Lin, Y., Ravikovitch, P.I., Thommes, M.: Quenched solid density functional theory and pore size analysis of micro-mesoporous carbons. Carbon **47**, 1617–1628 (2009)

Noh, J.S., Schwarz, J.A.: Estimation of the point of zero charge of simple oxides by mass titration. J. Colloid Interface Sci. **130**(1), 157–164 (1988)

Noh, J.S., Schwarz, J.A.: Effect of HNO_3 treatment on the surface acidity of activated carbons. Carbon **28**(5), 675–682 (1990)

Ouensanga, A., Largitte, L., Arsene, M.A.: The dependence of char yield on the amounts of components in precursors for pyrolysed tropical fruit stones and seeds. Micorporous Mesorporous Mater. **59**, 85–91 (2003)

Puziy, A.M., Poddubnaya, O.I., Martínez-Alonso, A., Suárez-García, F., Tascón, J.M.D.: Synthetic carbons activated with phosphoric acid I. Surface chemistry and ion binding properties. Carbon **40**, 1493–1505 (2002)

Puziy, A.M., Poddubnaya, O.I., Martínez-Alonso, A., Suárez-García, F., Tascón, J.M.D.: Surface chemistry of phosphorus-containing carbons of lignocellulosic origin. Carbon **43**, 2857–2868 (2005)

Ruddy, E.N., Carroll, L.A.: Select the best VOC control strategy. Chem. Eng. Prog. **89**, 28–35 (1993)

Salame, I.I., Bandosz, T.J.: Experimental study of water adsorption on activated carbons. Langmuir **15**, 587–593 (1999a)

Salame, I.I., Bandosz, T.J.: Study of water adsorption on activated carbons with different degrees of surface oxidation. J. Colloid Interface Sci. **210**, 367–374 (1999b)

Sillman, S.: Tropospheric ozone and photochemical smog. In: Heinrich, D., Hollan, Karl K. (eds.) Treatise on Geochemistry, vol 9, pp. 407–431. Elsevier, Turekian (2003)

Silvestre-Albero, A., Silvestre-Albero, J., Sepúlveda-Escribano, A., Rodríguez-Reinoso, F.: Ethanol removal using activated carbon: effect of porous structure and surface chemistry. Microporous Mesoporous Mater. **120**, 62–68 (2009)

Suárez-García, F., Martínez-Alonso, A., Tascón, J.M.D.: Activated carbon fibers from Nomex by chemical activation with phosphoric acid. Carbon **42**, 1419–1426 (2004)

Valente Nabais, J.M., Laginhas, C.E.C., Carrott, P.J.M., Ribeiro Carrott, M.M.L.: Production of activated carbons from almond shell. Fuel Process. Technol. **92**, 234–240 (2011)

Werner, M.D.: The effects of relative humidity on the vapour phase adsorption of trichloroethylene by activated carbon. Am. Ind. Hyg. Assoc. J. **46**(10), 585–590 (1985)